University of Glasgow

Wahler, M., Buttner, B., Blaschek, H.H., Homonnay, N., Wid, O., O'Shea, K.J., McGrouther, D., MacLaren, D.A., and Schmidt, G.(2014) *Controlling magnetic anisotropy in $La_{0.7}Sr_{0.3}MnO_3$ nanostructures.* Applied Physics Letters, 104 . 052408-1. ISSN 0003-6951.

Copyright © 2014 American Institute of Physics

A copy can be downloaded for personal non-commercial research or study, without prior permission or charge

Content must not be changed in any way or reproduced in any format or medium without the formal permission of the copyright holder(s)

When referring to this work, full bibliographic details must be given

http://eprints.gla.ac.uk/91182/

Deposited on: 17 February 2014

Enlighten – Research publications by members of the University of Glasgow
http://eprints.gla.ac.uk

This is an unedited, pre-submission (and therefore possibly incomplete) version of a manuscript that appears in full at http://dx.doi.org/10.1063/1.4863978. Please contact donald.maclaren@glasgow.ac.uk directly for a final version.

Controlling magnetic anisotropy in $La_{0.7}Sr_{0.3}MnO_3$ nanostructures

M. Wahler[1], B. Büttner[1], H.-H. Blaschek[1], N. Homonnay[1], O. Wid[1],

K.J. O'Shea[2], D. McGrouther[2], D.A. MacLaren[2], and G. Schmidt*[1,3]

[1]*Institut für Physik, Martin-Luther-Universität Halle-Wittenberg, D-06099, Germany**

[2]*SUPA, School of Physics and Astronomy,*

University of Glasgow, Glasgow G12 8QQ, UK

[3]*IZM, Martin-Luther-Universität Halle-Wittenberg, D-06099, Germany**

**present and permanent address G.S.*

Correspondence to G. Schmidt email: georg.schmidt@physik.uni-halle.de

Abstract

We have developed a chlorine based dry etching process that can be used to pattern the ferromagnetic oxide $La_{0.7}Sr_{0.3}MnO_3$ (LSMO). The process allows the creation of nanostructures with lateral dimensions down to 100 nm from epitaxial LSMO films without degradation of the magnetic properties. Large arrays of millions of identical structures have been fabricated from thin epitaxial LSMO films by electron-beam lithography and reactive ion etching and have been characterized by SQUID magnetometry. The processed structures retain the full magnetization and the Curie temperature of the bulk layer. High resolution scanning transmission electron microscopy (HRSTEM) shows that crystallinity is preserved even at the edges of the nanostructures.

This is an unedited, pre-submission (and therefore possibly incomplete) version of a manuscript that appears in full at http://dx.doi.org/10.1063/1.4863978. Please contact donald.maclaren@glasgow.ac.uk directly for a final version.

I. INTRODUCTION

Due to their potentially high spin polarization, ferromagnetic oxides are promising candidates for spintronics device applications [1]. A major prerequisite for application of any material in today's microelectronics, however, is the availability of suitable nanopatterning processes for the sub-100 nm regime. It is self-evident that these patterning processes must preserve all of the physical properties of the respective material that are relevant to the application. In the case of ferromagnetic oxides we therefore need a patterning process which does not diminish the magnetization or the Curie temperature. In view of modern fabrication techniques an anisotropic dry etching process is much preferred compared to wet chemical etching which is usually isotropic, but finding a process can prove difficult because the magnetic properties of epitaxial oxides strongly depend on the crystalline quality of the layers, which may degrade during dry etching. For the process development we have chosen LSMO because it is easily grown with reproducible quality and is also known to have a high spin polarization. It is well studied and its Curie temperature is above, but close to, room temperature. The Curie temperature is sensitive to crystalline damage and any change can easily be observed in the experiment [2].

In former experiments the influence of defects on magnetization has already been exploited for the creation of laterally constrained magnetic areas using masking and ion implantation which reduces magnetization rather than removing the material [2, 3]. These processes, however, only confine the magnetization but do not truly nanostructure the material which would be necessary for electrical device fabrication where electrical insulation is also an issue. One example for true geometrical patterning by etching was published by Wu *et al.* [4]. Using optical lithography and an unnamed patterning process, structures with lateral dimensions larger than 500 nm were fabricated from LSMO layers thicker than 45 nm. In these structures full magnetization was maintained. For feature sizes down to 100 nm, however, no suitable patterning process has been published so far. From semiconductor patterning, where similar problems exist, it is known [5] that purely physical processes like, such as argon ion beam etching, can be detrimental to electronic and optical properties, while processes with an additional chemical etching component yield much better results [6]. Here, we present the results of a physical/chemical dry etching process, focusing on the

This is an unedited, pre-submission (and therefore possibly incomplete) version of a manuscript that appears in full at http://dx.doi.org/10.1063/1.4863978. Please contact donald.maclaren@glasgow.ac.uk directly for a final version.

determination of the magnetic properties of the fabricated nanostructures.

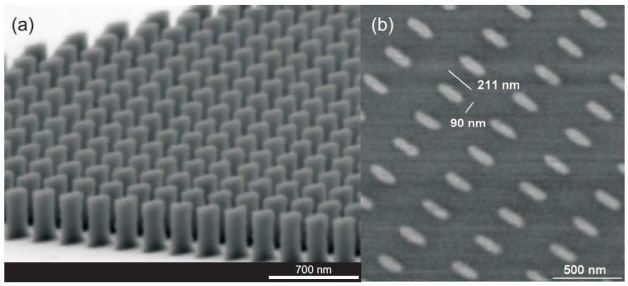

FIG. 1: SEM images of the nanopatterned sample showing (a) the resist mask and (b) the etched nanostructures after removal of resist.

II. SAMPLE PREPARATION AND MEASUREMENT TECHNIQUES

Our samples are fabricated from state-of-the-art quality LSMO films with deposited by pulsed laser depostition (PLD) on (001) oriented $SrTiO_3$ substrates (using an oxygen pressure of 0.2 mbar, substrate temperature of 700 °C, laser fluency of 3.5 J/cm^2, repetition rate of 5 Hz and a deposition time of 11:38 Minutes). The layer thickness is determined by RHEED oscillations during growth. Reciprocal space maps obtained by X-ray diffraction show that growth is epitaxial, pseudomorphic and that the layers are fully strained. X-ray reflectometry shows a typical RMS roughness of < 3 Å.

As mentioned before, we use electron-beam lithography and an Ar/Cl_2 inductively coupled reactive ion etching (ICP-RIE) process to pattern the samples. For the lithography, a novolac based resist with a thickness of 300 nm is spin-coated onto the as-grown sample. The resist is exposed by electron-beam lithography. Figure 1 (a) shows an SEM image of the resulting resist mask after development. The pattern is subsequently transferred by dry etching using an Oxford Plasmalab 100 System, yielding the structures shown in fig. 1 (b). The etching process uses a gas mixture of argon and chlorine with a ratio of 14:1 and a process pressure of 5 mTorr. The total plasma power is 1000 W (750 W ICP and 250 W RIE), giving an etch rate for LSMO of (19 ± 3) nm/min, with a selectivity of approximately 1:6 with respect to the resist. A process time of 1:53 min is thus sufficient to guarantee the full removal of the exposed 20 nm thick LSMO with a reasonable resist thickness remaining to protect the masked areas.

This is an unedited, pre-submission (and therefore possibly incomplete) version of a manuscript that appears in full at http://dx.doi.org/10.1063/1.4863978. Please contact donald.maclaren@glasgow.ac.uk directly for a final version.

On a single sample with a continuous homogeneous LSMO film we use this process to pattern three separate areas with different structures. The first area (sample 1) is left unmasked (no e-beam exposure). In this area all LSMO is removed during the etching process. This part of the sample is later used to identify any artefact or any additional magnetization that might be induced by handling, cutting, or etching. The second area (sample 2) holds the array of approximately 70 million rectangles with nominal lateral dimensions of 90 nm x 200 nm and a period of 295 nm along the short axis and 405 nm along the long axis of the rectangles. Post process scanning electron microscopy imaging reveals the nanostructures to have lateral dimensions of (105±10) nm by (225±15) nm. In the third area (sample 3) only a macroscopic square of LSMO is masked. The area of the square is equivalent to the effectively masked overall area of the nanorectangles. This last sample is used to compare the magnetization of macroscopic layers and nanostructures, respectively.

During the subsequent cutting process, which is necessary to separate the samples for individual measurement, a non-magnetic wire saw is used in order to avoid magnetic contamination. For all three resulting samples, the edges of the initial substrate are also removed, to guarantee that no signal emanates from LSMO that might have been deposited on the substrate side walls during the PLD process.

III. MEASUREMENT RESULTS AND DISCUSSION

The structural quality of the nanostructures was investigated by cross sectional high resolution scanning transmission electron microscopy (HRSTEM). The pictures show that the crystallinity of the sample is preserved even close to the surface exposed to the etching process (fig. 2).

The magnetic moment of all samples, respectively, is determined using a Quantum Design Inc. MPMS® SQUID VSM. The magnetization is measured of all samples during cool-down from 380 K to 4.2 K in a finite magnetic field of 1 kOe. The M(T) curve is corrected for a negative constant diamagnetic contribution from the substrate.

The measurement of the control sample (sample 1) with nominally no LSMO left (sample 1) shows a very small finite magnetization at low temperatures (figure 3), which is also seen in measurements on this type of substrate, prior to material deposition. As will be shown

This is an unedited, pre-submission (and therefore possibly incomplete) version of a manuscript that appears in full at http://dx.doi.org/10.1063/1.4863978. Please contact donald.maclaren@glasgow.ac.uk directly for a final version.

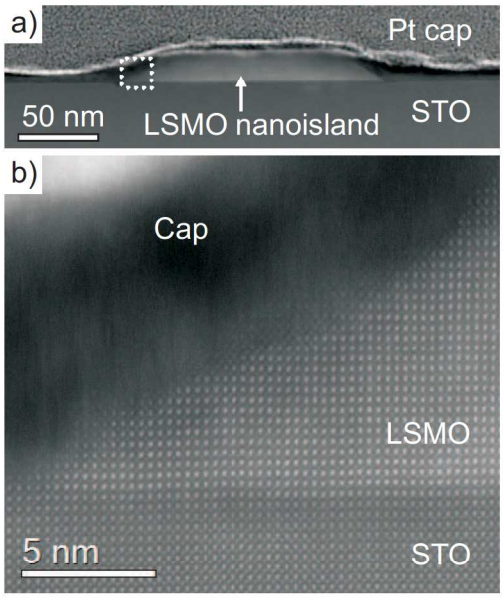

FIG. 2: Dark field scanning transmission electron microscopy images of the cross-section of a single nanoisland. (a) Low magnification image showing the island and capping layers. (b) High magnification image of the edge of an island, indicating that a good epitaxial relationship between island and substrate is maintained.

later this magnetization is smaller than even the error bars for the LSMO containing samples.

For the magnetic samples we measure the total magnetization value, taking into account the correction factors for the different sample geometries, which are inherent in the measurement system [7, 8]. Using the respective volume of the magnetic material we also determine the magnetization per Mn atom. It should be noted that the area of the large square (sample 3) can be determined with high precision as it is given by the error of the electron-beam lithography or, more precisely, the interferometer controlled sample stage. The layer thickness is determined by counting RHEED oscillations and has an error of approximately ± 0.4 nm corresponding to one monolayer. Only for the nanorectangles the lateral size must be determined using electron microscopy which is done by averaging over a number of different islands. We estimate the maximum total error to be 20%.

The magnetization versus temperature curves in figure 3 shows, that the Curie temperatures of the e-beam patterned nano array (black curve) and the reference large area square (red curve) are the same at $T_C = 350$ K. The large square of LSMO has a magnetization per Mn atom which is below the maximum bulk value determined from the literature [9] but still

This is an unedited, pre-submission (and therefore possibly incomplete) version of a manuscript that appears in full at http://dx.doi.org/10.1063/1.4863978. Please contact donald.maclaren@glasgow.ac.uk directly for a final version.

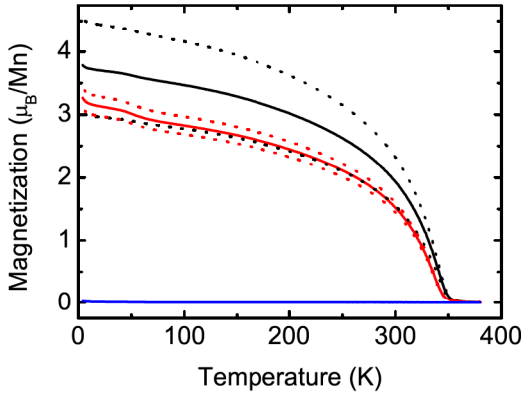

FIG. 3: Field-cooled magnetization versus temperature curves at $B = 1$ kOe (i.e. in saturation) measured with SQUID. The dotted lines indicate the maximum estimated error margin. The black curve shows the magnetization of the e-beam-patterned nanoarray (sample 2). The red curve shows the data from the reference sample (sample 3) with an unpatterned LSMO film of nominally the same magnetic volume. The blue curve shows the measurement of the second reference sample, a sample of 5 mm x 2 mm from which all LSMO is removed.

shows reasonable material properties. The measurements also clearly show that the magnetization of the nanostructures has not decreased within the error bars. Interestingly, the magnetization of the nanopatterned LSMO even seems to have increased in comparison to the large area value. Due to the large error bars we cannot prove that this increase is due to a change in magnetization, nevertheless, this tendency is systematic in all nanoarrays that we have fabricated so far. Although more experiments are necessary to confirm the effect, a possible explanation might be the following: using bulk lattice parameters of $a_{\mathrm{LSMO}} \approx 3.876$ Å and $a_{\mathrm{STO}} \approx 3.905$ Å the lattice mismatch is $\delta = (a_{\mathrm{STO}} - a_{\mathrm{LSMO}})/a_{\mathrm{STO}} \approx 0.74\%$. From reciprocal spacemaps, we see that the unpatterned LSMO layer is fully strained. Thiele *et al.* have shown that the magnetization of LSMO changes with in-plane strain [10]. Therefore, patterning a strained layer can lead to elastic strain relaxation which modifies the magnetic properties as has also been observed in (Ga,Mn)As nanostructures [11].

On samples 2 and 3 we have also measured hysteresis loops with the magnetic field applied in various directions at a temperature of 4.2 K. From ferromagnetic resonance measurements (FMR) we know that at this temperature the LSMO exhibits a biaxial anisotropy with magnetic easy axes parallel to [110] and [1$\bar{1}$0] [12]. The anisotropy field as obtained from

This is an unedited, pre-submission (and therefore possibly incomplete) version of a manuscript that appears in full at http://dx.doi.org/10.1063/1.4863978. Please contact donald.maclaren@glasgow.ac.uk directly for a final version.

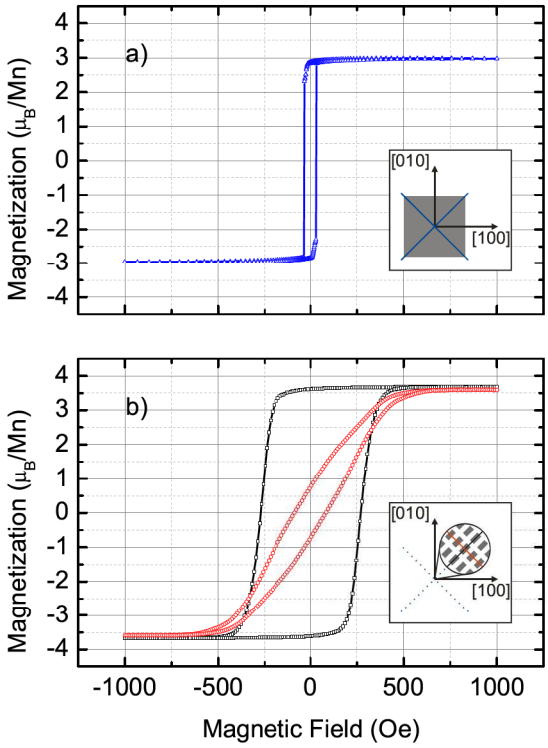

FIG. 4: Hysteresis loops at $T = 4.2$ K with the linear diamagnetic contribution from the STO substrate subtracted. Error bars are omitted for clarity, but the same uncertainties apply as in Fig. 3. a) Magnetization of the reference sample with an unpatterned film of nominally the same LSMO volume, measured along one of the two magnetic easy axes. b) Magnetization along long side of the rectangles (black) showing an easy axis signature and short side (red) with hard axis behavior, as expected from shape anisotropy. Note that both directions correspond to the easy magnetic directions of the as-grown LSMO layer. Coercive fields are increased in the nanopatterned sample due to the domain wall formation energy.

FMR is at least 350 Oe. For the hysteresis loop of sample 3 (large square) the magnetic field is applied in-plane along the easy axis.

Figure 4 (a) shows the hysteresis loop for the square sample. The coercive field is 32 Oe. At reversal the magnetization goes almost to full saturation as can be expected for an easy axis. The rectangular nanostructures are aligned with their edges along the two easy axes of the LSMO on the nanopatterned sample (figure 4 (b)). In the hysteresis loops taken along

This is an unedited, pre-submission (and therefore possibly incomplete) version of a manuscript that appears in full at http://dx.doi.org/10.1063/1.4863978. Please contact donald.maclaren@glasgow.ac.uk directly for a final version.

these two axes we can observe several effects of the nanopatterning. Firstly, we observe again an easy axis behavior for the magnetic field applied along the long edges of the rectangles. This is to be expected because here shape anisotropy should emphasize the easy axis. The coercive field, however, is much larger than for the macroscopic square sample. The reason for this is the increasing domain wall nucleation energy in nanostructures, which hinders the magnetization reversal and shifts the coercive field closer to pure Stoner rotation [13]. The coercive field, however, is still slightly lower than the shape anisotropy field along the short axis of the rectangles. In addition we do not observe a sharp switching event but a reversal of the rectangles over a field range of almost 200 Oe. This is readily explained by small size variations and edge roughness of the nanostructures which change lead to a variation of the domain wall nucleation energy and thus the respective coercive fields. When the magnetic field is applied along the short axis of the rectangles we observe the signature of a hard axis. The hysteresis loop is barely open and it takes much higher fields to achieve full saturation. Here, the shape anisotropy is even stronger than the crystalline anisotropy of the epitaxial layer and it favors magnetization along the elongated structures. In total, the magnetization of the nanostructures is now mainly dominated by the nanopatterning rather than by the original anisotropy of the layer.

IV. CONCLUSION

We have fabricated LSMO nanostructures by electron-beam lithography and reactive ion etching. The magnetization measurements clearly show that the magnetic properties do not degrade during the etching step and, indeed, may increase via strain relaxation. We have also shown that by nanopatterning we can create structures with a coercive field and anisotropy different from those of the original layer.

This is an unedited, pre-submission (and therefore possibly incomplete) version of a manuscript that appears in full at http://dx.doi.org/10.1063/1.4863978. Please contact donald.maclaren@glasgow.ac.uk directly for a final version.

Acknowledgments

We acknowledge the support of this work by the DFG in the SFB762 and by the EC in the FP7 project IFOX, grant n° NMP3-LA-2010-246102.

---

[1] N. V. Volkov, Physics-Uspekhi **55**, 250 (2012).

[2] Y. Takamura, R. V. Chopdekar, A. Scholl, A. Doran, J. A. Liddle, B. Harteneck, and Y. Suzuki, Nano Letters **6**, 1287 (2006).

[3] E. Kim, J. Watts, B. Harteneck, A. Scholl, A. Young, A. Doran, and Y. Suzuki, Journal of Applied Physics **109**, 07D712 (2011).

[4] Y. Wu, Y. Matsushita, and Y. Suzuki, Phys. Rev. B **64**, 220404 (2001.

[5] T. J. Cotler and M. E. Elta, Circuits and Devices Magazine, IEEE **6**, 38 (1990).

[6] T. Kummell, G. Bacher, A. Forchel, J. Nurnberger, W. Faschinger, G. Landwehr, B. Jobst, and D. Hommel, Appl. Phys. Lett. **71**, 344 (1997).

[7] M. Sawicki, W. Stefanowicz, and A. Ney, Semiconductor Science and Technology **26**, 064006 (2011).

[8] *SQUID VSM Application Note 1500-015: Accuracy of the Reported Moment: Sample Shape Effects*, Quantum Design Inc. (2010).

[9] Y. Tokura and Y. Tomioka, Journal of Magnetism and Magnetic Materials **200**, 1 (1999).

[10] C. Thiele, K. Dorr, O. Bilani, J. Rodel, and L. Schultz, Physical Review B **75**, 054408 (2007).

[11] J. Wenisch, C. Gould, L. Ebel, J. Storz, K. Pappert, M. J. Schmidt, C. Kumpf, G. Schmidt, K. Brunner, and L. W. Molenkamp, Phys. Rev. Lett. **99**, 077201 (2007).

[12] M. Mathews, F. M. Postma, J. C. Lodder, R. Jansen, G. Rijnders, and D. H. A. Blank, Applied Physics Letters **87**, 242507 (2005).

[13] E. Stoner and E. Wohlfarth, Philosophical Transactions of the Royal Society of London. Series A. Mathematical and Physical Sciences pp. 599–642 (1948).